Geophysical Research Letters

RESEARCH LETTER
10.1029/2018GL081620

The Origin of Carbonate Mud

Elizabeth J. Trower[1], Michael P. Lamb[2], and Woodward W. Fischer[2]

[1]Department of Geological Sciences, University of Colorado Boulder, Boulder, CO, USA, [2]Division of Geological and Planetary Sciences, California Institute of Technology, Pasadena, CA, USA

Key Points:
- Experiments demonstrate that abrasion of carbonate sand generates carbonate mud at geologically significant rates
- An abrasion rate model can be used to estimate fluxes of carbonate mud produced via abrasion in modern and ancient environments
- Abrasion-produced mud may reflect a mixture of carbonate particles of varying age and composition

Supporting Information:
- Supporting Information S1

Correspondence to:
E. J. Trower,
lizzy.trower@colorado.edu

Citation:
Trower, E. J., Lamb, M. P., & Fischer, W. W. (2019). The Origin of Carbonate Mud. *Geophysical Research Letters*, *46*. https://doi.org/10.1029/2018GL081620

Received 10 DEC 2018
Accepted 12 FEB 2019
Accepted article online 15 FEB 2019

Abstract Carbonate mudstones are key geochemical archives for past seawater chemistry, yet the origin of carbonate mud remains a subject of continued debate and uncertainty. Prevailing hypotheses have settled on two mechanisms: (1) direct precipitation in the water column and (2) postmortem dispersal of mud-sized algal skeletal components. However, both mechanisms conflict with geochemical observations in modern systems and are problematic in deep time. We tested the hypothesis that abrasion of carbonate sand during sediment transport might produce carbonate mud using laboratory experiments and a sediment transport model. We documented experimental mud production rates up to two orders f magnitude faster than rates estimated for other mechanisms. Combined with model calculations, these results illustrated that transport and abrasion of carbonate sand is a major source of carbonate mud.

Plain Language Summary Carbonate mudstones are widely used as archives of ancient seawater chemistry, under the assumption that the compositions of mud-sized (<62.5 μm in diameter) carbonate particles that make up these mudstones provide reliable records of seawater at the time the particles were formed and deposited. This assumption relies on understanding how carbonate mud forms—current ideas center on direct mineral precipitation from seawater and the disintegration of algae mineral skeletons—but these mechanisms conflict with some geochemical observations in modern systems. We used experiments to demonstrate that when carbonate sand grains are transported by currents, collisions cause mud-sized carbonate particles to be released from grain surfaces via abrasion. The rapid rates of carbonate mud production observed in our experiments suggest that abrasion has been a significant source of carbonate mud throughout Earth history, which is important for interpreting geochemical records from carbonate mudstones because the material abraded from sand grains may not be instantaneous records of seawater chemistry.

1. Introduction

Carbonate mud (particle diameter <62.5 μm) is a major sedimentary component of modern carbonate environments and the ancient carbonate rock record and forms one of the largest sinks in the geological carbon cycle, particularly prior to the evolution of carbonate-biomineralizing organisms (Grotzinger & James, 2000; Pomar & Hallock, 2008). Carbonate mudstones and wackestones are also significant geochemical archives and petroleum source rocks (Palacas et al., 1984). Nevertheless, the origin of carbonate mud remains enigmatic, reflecting a knowledge gap in carbon cycle fluxes and the interpretation of carbonate geochemical records. Much of the debate on the origin of carbonate mud has focused on two mechanisms: (1) primary precipitation of aragonite in the water column, whether via homogeneous precipitation (Cloud et al., 1962; Macintyre & Reid, 1992; Milliman et al., 1993; Shinn et al., 1989) or nucleated on suspended carbonate particles (Morse et al., 2003) or microbes (Robbins & Blackwelder, 1992; Yates & Robbins, 1998), and (2) postmortem disintegration and dispersal of the skeletons of calcifying organisms —particularly calcareous algae and foraminifera—into individual mud-sized carbonate particles (Broecker et al., 2000; Broecker & Takahashi, 1966; Debenay et al., 1999; Lowenstam, 1955; Nelsen & Ginsburg, 1986; Neumann & Land, 1975; Stockman et al., 1967). Both mechanisms conflict with geochemical observations of modern carbonate mud: radiocarbon data preclude water column precipitation (Broecker et al., 2000; Broecker & Takahashi, 1966), while Sr concentration data are inconsistent with algal production (Milliman et al., 1993). Bioerosion has also been suggested as a significant mode of mud production (Farrow & Fyfe, 1988; Hallock, 1988), but both bioerosion and the algal mechanisms do not extend prior to the evolution of these organisms. The current paradigm therefore requires that, for the majority of Earth history, mud production occurred exclusively through water column precipitation, even though recent work on the Great Bahama Bank has shown that this mechanism appears to

require not only favorable seawater chemistry but also a particular pattern of water circulation (Purkis et al., 2017). Over a hundred years ago, Sorby (1879) originally suggested that mechanical breakdown of carbonate sand might represent a significant source of carbonate mud; this idea has not been tested, but it could potentially resolve conflicts with geochemical data and augment the Precambrian carbonate mud budget.

Recent wet abrasion mill experiments demonstrated that abrasion rates of ooids—a type of nonskeletal carbonate sand—are rapid under transport conditions typical in shoal environments (Trower et al., 2017). Similarly, tumbling barrel experiments have shown that breakdown of skeletal carbonate can be rapid (Ford & Kench, 2012)—the mud-sized products of which have been identified in modern carbonate muds (Gischler & Zingeler, 2002). In addition to polishing grain surfaces (Trower et al., 2017, 2018), this mechanical abrasion of sand-sized particles produces finer material at a volumetric rate equal to the volumetric rate of sand diminution. In this study, we constructed a model to estimate the rate of production of carbonate mud via abrasion of coarser particles as a function of sand grain size and sediment transport mode by modifying a recent ooid abrasion rate model (Trower et al., 2017). We then designed a series of wet abrasion mill experiments to examine the size, shape, and production rates of carbonate particles produced by abrasion of carbonate sand for a range of grain sizes and transport modes spanning plausible fair weather and storm conditions. We compared these experimental and model rates of mud production via abrasion to existing estimates of carbonate mud production rates by other mechanisms to test the hypothesis that mechanical abrasion of carbonate sand is a significant source of carbonate mud in both modern and ancient carbonate environments.

2. Materials and Methods

2.1. Abrasion Model

We designed a model to predict the rate of mud production via abrasion of sand-sized particles, dV_m/dt, based on bedrock erosion models (Lamb et al., 2008; Sklar & Dietrich, 2004), which account for bed erosion resulting from the frequency and energy of particle impacts with the bed as a function of bed shear velocity (u_*) and grain size (D), and a recent abrasion model that applied these principles to the diminution of carbonate sand grains—specifically, ooids—during transport (Trower et al., 2017). Bed shear velocity can be related to current and wave properties in coastal settings (Grant & Madsen, 1982) and, in combination with grain size, can be used to estimate sediment transport mode using the dimensionless Rouse number, $P = w_s/(\kappa u_*)$, where $\kappa = 0.41$ is von Kármán's constant and w_s is sediment fall velocity, which can be calculated as a function of D, densities of the fluid (ρ_f) and sediment (ρ_s), and kinematic fluid viscosity (ν) following Dietrich (1982). In the ooid abrasion model (Trower et al., 2017), which follows bedrock erosion models (Lamb et al., 2008; Sklar & Dietrich, 2004), volumetric abrasion rate (dV_p/dt) is the product of the volume eroded per impact (V_i) and the impact rate (I_r) for a single particle: $dV_p/dt = V_i I_r$. We assumed that the volumetric rate of particle diminution (dV_p/dt) is proportional to the volumetric rate of mud production through abrasion (dV_m/dt): $dV_m/dt = -k_m\, dV_p/dt$, where k_m is the fraction of total material lost by sand abrasion, dV_p/dt, that results in the production of mud-sized ($D < 62.5$ μm) particles, dV_m/dt, with the remainder to very-fine-sand-sized (62.5 μm $< D <$ 125 μm) particles produced by fragmentation (Le Bouteiller et al., 2011). The volume eroded per impact is defined following Sklar and Dietrich (2004) as

$$V_i = \frac{1}{2}\frac{V_p \rho_s w_i^2}{\varepsilon_v} \tag{1}$$

where V_p is particle volume, ρ_s is particle density (2.8 g/cm^3), w_i is impact velocity normal to the bed calculated following Lamb et al. (2008; see Text S1 in the supporting information), and ε_v is the kinetic energy per unit volume eroded, defined as

$$\varepsilon_v = k_v \frac{\sigma_T^2}{2Y} \tag{2}$$

where σ_T is the tensile strength (10^6 kg/m/s^2) and Y is Young's modulus (1.44×10^{11} kg/m/s^2), which were set following Trower et al. (2017), and $k_v \approx 10^6$ is a dimensionless coefficient that accounts for differences in material properties between the particles and the bed surface (Scheingross et al., 2014).

The ooid abrasion model considers the impact rate for a single particle (Trower et al., 2017), while for mud production we considered the combined effects of many active particles interacting with the bed. Therefore, we followed the impact rate formulation in Lamb et al. (2008), which accounts for the near-bed volumetric concentration, c_b:

$$I_r = \frac{A_1 c_b w_s}{V_p} \tag{3}$$

where $A_1 = 0.3$ is a dimensionless coefficient, V_p is particle volume, and c_b is calculated to be at the transport capacity limit following Garcia and Parker (1991), which is appropriate for natural sandy beds:

$$c_b = E = \frac{AZ^5}{1 + \frac{A}{0.3} Z^5} \tag{4}$$

where E is a dimensionless ratio describing the entrainment of sediment from the bed into suspension, $A = 1.3 \times 10^{-7}$ is an empirical constant, and Z is a dimensionless variable defined as

$$Z = \frac{u_*}{w_s} \mathrm{Re}_p^{0.6} \tag{5}$$

where $\mathrm{Re}_p = \frac{\sqrt{RgD}D}{\nu}$ is a particle Reynolds number in which ν is kinematic fluid viscosity (which was 1.3×10^{-6} m^2/s for our experiments), $R = \frac{\rho_f - \rho_s}{\rho_f}$ is submerged specific density of sediment ($\rho_f = 1.025$ g/cm^3 is fluid density), and g is the acceleration due to gravity.

2.2. Experimental Methods

We designed a series of experiments to determine carbonate mud production rates as a function of grain type, grain size, and bed shear velocity using a series of wet abrasion mills similar to those employed in bedrock erosion (Scheingross et al., 2014; Sklar & Dietrich, 2001) and ooid abrasion experiments (Trower et al., 2017; Figure S1). Two representative carbonate sand types were selected: natural marine ooids collected from Ambergris Shoal in the Turks and Caicos Islands and marine skeletal carbonate sand commercially available as CaribSea Fiji Pink Reef Sand aquarium substrate. Both types of carbonate sand were sieved to produce subsamples with a range of median grain sizes (D_{50}). Due to the well-sorted character of natural ooid sands, the Ambergris ooids yielded only two size fractions with D_{50} of 417 and 558 μm, while the Fiji Pink skeletal sand yielded four size fractions with D_{50} of 450, 635, 860, and 1144 μm. A series of abrasion experiments was run for each of the grain type/size populations at a constant propeller speed, using a hardground of ooids epoxied to the base of the mill as the abrasive surface and an artificial seawater fluid mixed using CoraLife aquarium salt, which is slightly supersaturated with respect to aragonite (Atkinson & Bingman, 1997). An additional set of trials was also run using variable propeller speeds with a constant grain type/size to examine the relationship between bed shear velocity and mud production rate. For all experiments, bed shear velocity (u_*) was above the threshold of motion for the coarsest grains, and it was visually confirmed that all grains were in motion for all experiments; u_* was calibrated following previous abrasion mill experiments (Scheingross et al., 2014; Sklar & Dietrich, 2001; Trower et al., 2017). The sediment supply was set to be just under the transport capacity of the flow to eliminate the added complexity of grain exchange between an active transport layer and a static alluviated bed; c_b was calculated assuming transport limited conditions (equation (4)). The range of experimental conditions was chosen to bracket typical fair weather and storm conditions for grainy, current-agitated settings on carbonate platforms (Rankey & Reeder, 2010). In all experiments, the cloud of suspended sand-sized sediment was far below the propeller in the abrasion mill such that there were no grain-propeller impacts. Sediment concentrations were dilute such that grain-grain collisions in the water column were negligible relative to grain-bed impacts (Kench, 1998; Leeder, 1979). The experiments were conducted using a set of three abrasion mills running in series. Each set of three experiments included two sand-present mills and one sand-free mill with the same artificial seawater and propeller speed to control for the possibility that any carbonate precipitated from the fluid. Experiment parameters are provided in Table S1.

Two independent methods were used to characterize mud production rate for each experiment: a direct measurement of suspended mud concentration and a measurement of the change in grain size of carbonate sand

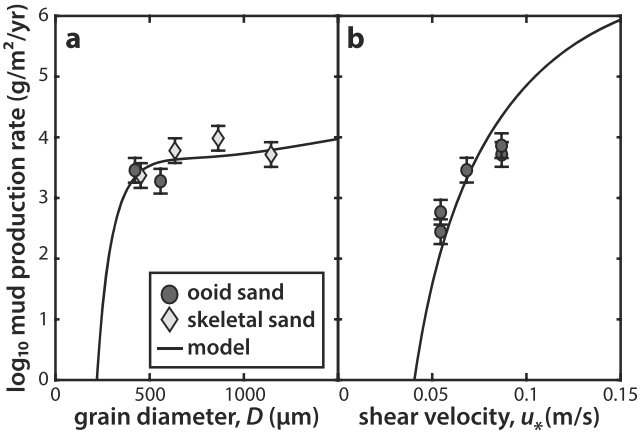

Figure 1. Experimental mud production rates by abrasion of carbonate sand during sediment transport compared with calibrated model predictions. (a) Mud production rates as a function of initial grain size for both ooid (dark gray circles) and skeletal carbonate sand (light gray diamonds) for a fixed bed shear velocity. (b) Mud production rates as a function of bed shear velocity for ooid sand with a fixed grain size, $D_{50} \approx 417$ μm. Error bars depict log error based on maximum variability between duplicate trials.

due to abrasion. To determine the mud concentration, 50-ml aliquots of water with suspended mud were collected from the middle of the water column in each mill immediately after stopping the propellers (to minimize settling). These aliquots were centrifuged at 3,000 rpm for 2 min and rinsed with deionized water—this procedure was repeated three times; after the third spin-down, the supernatant was drawn off with a pipette, and the samples were air-dried. The masses of dried mud samples were extrapolated to estimate a mud mass for the full abrasion mill volume (15.7 L), making the assumption of a constant concentration of mud throughout the water column. To determine the change in sand grain size, the size distribution of each sand sample was analyzed using a Retsch Camsizer P4 prior to each experiment. At the conclusion of each experiment, sand was recovered from each mill and rinsed using 62-μm wire mesh. Dried sand samples were reanalyzed with the Camsizer. Using the Camsizer data, the change in sand size resulting in mud production (i.e., dV_m/dt) and the proportion of abrasion resulting in mud production (k_m) were calculated by subtracting the increase in volume of the very-fine-sand-size grains produced via fragmentation from the overall decrease in volume of sand-sized grains (Figure S2 and Table S2). Mud production rates are reported as the average of these two independent measurement methods and uncertainty based on maximum variability between duplicate trials, which is larger than the uncertainty between measurement methods.

Scanning electron microscopy (SEM) was used to compare the size and shape of carbonate mud particles produced in different trials. Additional aliquots of suspended mud were collected, rinsed, and dried as described above, using a slower 1,500-rpm centrifuge speed. Dried samples were smeared on carbon tape on aluminum stubs and carbon-coated prior to analysis via Zeiss 1550VP Field Emission SEM at the Caltech GPS Division Analytical Facility, using 13- to 16-mm working distance and 15-keV accelerating voltage. Particle sizes of experimentally produced carbonate mud samples were analyzed via CILAS 1190 laser particle size analyzer. Some samples were below the detection limit due to low experimental yields.

Experimental abrasion rates were used to calibrate two model parameters: k_m (the efficiency of mud production) and k_v; k_m was set as 0.92, the average of experimental results (range 0.80–0.98, standard deviation 0.07); k_v was set as 2.5×10^7, which optimized the model fit to experimental results (Figure S3).

3. Results

Wet abrasion mill experiments produced observable carbonate mud—the water columns were turbid and milky—in measurable quantities at rates ranging from 282–2.65×10^4 g/m^2/year (Table S1). Sand-free control experiments generated no qualitatively observable or quantitatively measurable carbonate, indicating that no direct precipitation from the water column occurred. This conclusion was further supported by comparing measurements of sand grain volume reduction with direct measurement of mud mass—the abrasion rates determined via mud mass were similar to or slightly less than the rates determined via change in sand grain size, demonstrating that additional direct precipitation onto abrasion-produced mud particles was negligible. With all else held equal, larger grain sizes corresponded with slightly larger mud production rates (Figure 1a), and increasing bed shear velocity corresponded with increased mud production rates (Figure 1b).

Abrasion of ooids produced mud that dominantly composed of aragonite needles 1–2 μm long and 100–200 nm wide (Figure 2a). Abrasion of skeletal sand produced a more heterogeneous mixture of particle shapes and sizes including much larger (>5 μm long and >1 μm wide) and much smaller (<500 nm long and <100 nm wide) needles as well as more equant nanoparticles with typical diameters of 100–200 nm (Figure 2b). The dimensions and shapes of mud particles produced experimentally by abrading natural marine ooids were indistinguishable from carbonate mud filtered from seawater collected at the same field site and were comparable to the aragonite needles that define the fabric of the ooid cortices (Figure S4). Similarly, the heterogeneity of particle dimensions and shapes produced by abrasion of skeletal carbonate

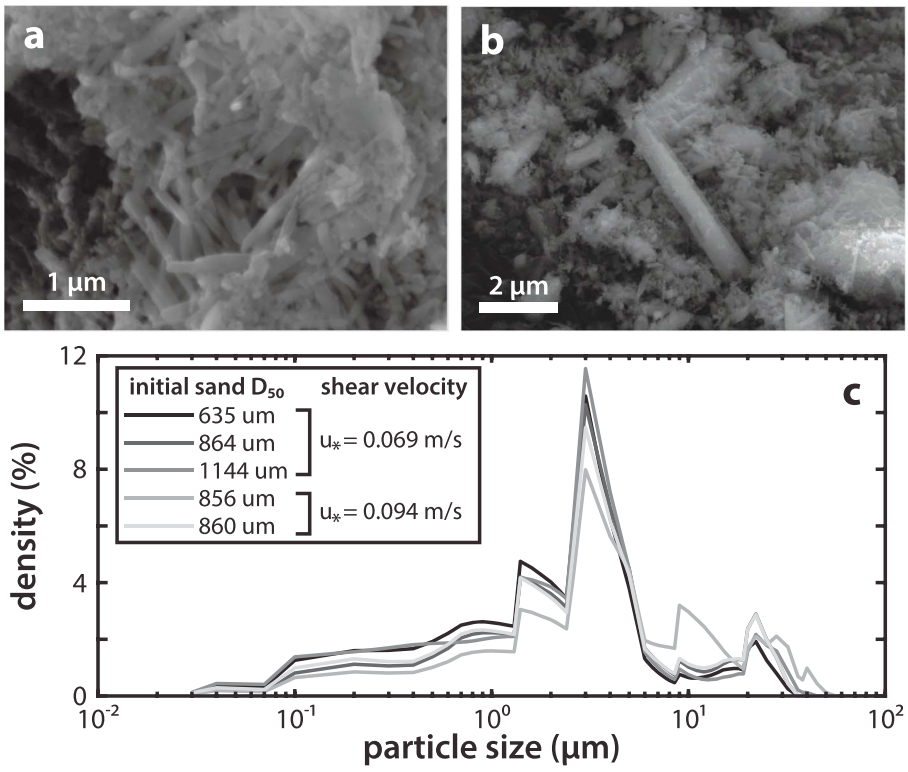

Figure 2. Scanning electron microscopy images of carbonate mud particles produced during sediment transport experiments. (a) Abrasion of natural marine ooids produced a relatively homogeneous population of aragonite needles 1–2 µm long and 100–200 nm wide. (b) Abrasion of skeletal carbonate sand produced a heterogeneous population of needles and equant particles with a wider range of sizes. (c) Particle size distributions for the carbonate mud produced from five trials using skeletal carbonate sand with varying initial grain sizes and shear velocities demonstrated consistency across experimental conditions with sand composition held constant.

send resembles carbonate mud from Florida Bay (Schieber et al., 2013) and other settings dominated by skeletal grains rather than ooids (Gischler et al., 2013). Laser-diffraction particle size analyses of the carbonate mud confirmed SEM observations that distributions of particle sizes were most sensitive to the initial sand composition rather than sand size or transport mode (Figure 2c).

The abrasion mud production model fit the experimental data well (Figures 1 and S3) using similar parameters as in the ooid abrasion model (Trower et al., 2017) and $k_m \approx 0.92$ (derived from experimental results). This k_m value implies that most of the material abraded from carbonate sand was mud sized (Table S2). The model predicts an increase in mud production with shear velocity due to more frequent and more energetic particle-bed impacts at higher shear velocities. Mud production rate is less sensitive to grain size because the more energetic impacts of larger grains—due to their greater masses and higher settling velocities—are offset by lower sediment concentrations and lower impact rates. Previous studies have estimated platform-averaged mud production rates ranging from 90–1000 g/m^2/year for algae and foraminifera (Debenay et al., 1999; Nelsen & Ginsburg, 1986; Neumann & Land, 1975) and 300–500 g/m^2/year for abiotic precipitation (Broecker & Takahashi, 1966; Milliman et al., 1993; Robbins et al., 1997). Our calibrated abrasion model predicted that grains >~600 µm in bed load and grains >~300 µm in suspended load would produce carbonate mud at rates equal to or faster than these other mechanisms (Figure 3).

4. Discussion

Our experimental data demonstrated that abrasion of carbonate sand under transport conditions typical of high-energy shoal environments produces carbonate mud at considerable rates. In many cases, experimental and model abrasion mud production rates are orders of magnitude faster than algal or precipitative mud production (Figure 3). This indicated that high-energy transport of carbonate sand—on a shoal or beach, for

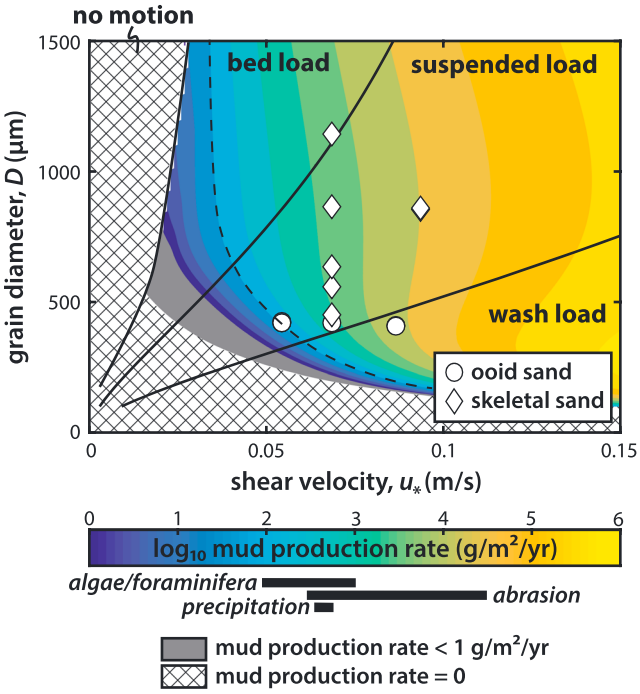

Figure 3. Contour plot of log mud production rates predicted by a calibrated abrasion model as a function of grain diameter and bed shear velocity. Experimental conditions are shown for ooid (circles) and skeletal (diamonds) carbonate sand. Boundaries between sediment transport modes are depicted by solid black lines. Ranges of estimated mud production rates for biological (algae and foraminifera; Debenay et al., 1999; Nelsen & Ginsburg, 1986; Neumann & Land, 1975) and chemical (precipitation and whitings; Broecker & Takahashi, 1966; Milliman et al., 1993; Robbins et al., 1997) mud production mechanisms are shown for comparison with the range of rates observed in our experiments. The area to the right of the dashed black line indicates combinations of grain diameter and bed shear velocity that the model predicts would produce carbonate mud at a rate equal to or faster than biological and chemical mechanisms. The gray and crosshatched areas indicate conditions for which the model predicts mud production rate <1 g/m^2/year or zero mud production, respectively. The sharp decline in abrasion rate for the finer grain sizes is predicted due to viscous damping of impacts using a Stokes threshold of $St_c = 10$ following Trower et al. (2017).

example—can produce fluxes of mud comparable to these other mechanisms even over smaller areas of carbonate platforms. Intermittency of grain movement, in particular when grains are trapped within bedforms, plays a role in diminishing the effective abrasion rate of carbonate sand over long timescales (Davies et al., 1978; Trower et al., 2017). However, typical bed shear velocities in many high-energy environments, like shoals, are persistently above the threshold for motion for the carbonate sand (Bathurst, 1975; Gonzalez & Eberli, 1997; Rankey et al., 2006), such that the production of mud by abrasion is not affected by the same intermittency factor as the abrasion of any individual sand grain. In quieter and/or deeper environments where fair weather conditions are below the threshold of motion, the production of mud through abrasion would be subject to the intermittency of bed shear velocities sufficient to transport sediment (e.g., storms). Large storms, like hurricanes, although occurring relatively infrequently, could generate mud at a fast rate for a short period of time by transporting grainy sediment in suspension over the area of an entire carbonate platform. For example, recent estimates suggest that the Great Bahama Bank is >65% grainy sediment (Harris et al., 2015). If this sediment is moved near the threshold of washload for 1 day by one hurricane per year, mud produced by abrasion during a hurricane could account for ~4% of the yearly mud production budget as estimated by Robbins et al. (1997; supporting information Text S2). In contrast, fair weather abrasion of the ~45% of the platform covered by "grainstone" facies (Harris et al., 2015) can account for 36% of the annual mud budget at our slowest experimental rate (supporting information Text S21). The true platform-averaged rate is likely to be higher considering the increased abrasion rate in more energetic settings like shoals and contributions from areas covered by "packstone" facies. Fair weather mud production by abrasion is therefore likely to be more significant than storm production over long timescales.

The observation of slow settling of whitings—regions of cloudy water defined by increased concentrations of suspended carbonate mud—has been cited as evidence that aragonite must be actively precipitating in the water column to replenish the suspended whiting cloud (Robbins et al., 1997; Shinn et al., 1989). Our experimental observations of mud particle size and shape can be used to calculate reasonable bounds on particle settling velocities; these range from 10^{-7} m/s for single particle settling to 10^{-4} m/s for a high degree of flocculation and large floccules (supporting information Text S3), indicating that suspension settling times on the order of days are reasonable for carbonate mud produced and suspended by currents strong enough to transport and abrade sand grains. Settling velocity also can be used to calculate a characteristic advection length scale—the horizontal distance over which a particle is transported by the flow before returning to the bed (Ganti et al., 2014). The ratios of advection length scales for carbonate mud or mud flocs to carbonate sand suggest that carbonate mud particles should travel 10^3 to 10^6 times as far as the sand grains from which they were originally produced (supporting information Text S3). One can therefore expect to find carbonate mud produced by abrasion kilometers to tens of kilometers distant from the current-agitated, grainy patches of seafloor on which it originated without requiring resuspension. Such a pattern is consistent with the spatial separation of grainy and muddy zones on modern carbonate platforms (Harris et al., 2015; Robbins et al., 1997) and the suggestion that whiting events might be related to Langmuir circulation (Dierrsen et al., 2009).

Our results demonstrate that abrasion is likely a significant source of carbonate mud on modern carbonate platforms: platforms like the Great Bahama Bank or the Caicos platform are dominated by grainy sediments, and currents that are typically strong enough to transport—and therefore abrade—those grains (Dravis & Wanless, 2017; Harris et al., 2015; Purkis et al., 2017; Robbins et al., 1997). Furthermore, we posit that the

carbonate mud within whitings could plausibly form via abrasion rather than water column precipitation or resuspension. If correct, this finding would resolve several contradictory observations: mud produced via abrasion can have old radiocarbon ages (Broecker et al., 2000) inherited from sand grains, higher Sr contents than algal aragonite (Milliman et al., 1993), the diversity of particle morphologies depending on the primary sand composition, long transport distances from the location of origin, and slow settling velocities such that particles remain in suspension for days. Similarities between $\delta^{13}C$ and $\delta^{18}O$ values and Sr concentrations of ooids and whitings in the Bahamas have previously been used to argue for whiting formation via water column precipitation (Milliman et al., 1993), but these data, combined with the old radiocarbon ages of whitings, are equally consistent with abrasion of ooids and other carbonate sand as a source of whiting mud. Although the carbonate in ooids is ultimately sourced from seawater dissolved inorganic carbon, the key difference between mud precipitated directly from seawater and mud produced via abrasion is its age—modern marine ooid cortices integrate hundreds to thousands of years of time (Beaupré et al., 2015; Duguid et al., 2010), with the consequence that mud particles abraded from ooids need not match the geochemistry of seawater at the time of their production. In other words, mud produced by abrasion—of ooids, skeletal grains, or other carbonate particles—would reflect a geochemical signal that integrates as much time as the grainy particles themselves, rather than an instantaneous snapshot of seawater dissolved inorganic carbon that would be expected from water column precipitation. Geochemical records from carbonate mudstones may therefore incorporate previously unrecognized biases dependent on the relative contribution of mud produced by abrasion and the composition of grainy source material (e.g., particle type, age, stable isotope, and trace element geochemistry).

The consistency of abrasion rates between particle types in our experiments suggests that abrasion of all carbonate grains, including not only ooids and skeletal grains but also peloids, hardground clasts, and other carbonate lithoclasts, would produce carbonate mud at geologically relevant rates. It is therefore likely that mud production via abrasion has been an important source of carbonate mud throughout Earth history, relaxing the reliance on seawater carbonate chemistry to drive mud production during much of geologic time and implying that temporal trends in carbonate mudstone abundance may not reflect variations in seawater carbonate saturation.

Acknowledgments
Lydia Kivrak assisted with abrasion mill experiments as part of a Summer Undergraduate Research Fellowship at the California Institute of Technology. We thank Brian Fuller and Tom Ulizio for assistance with abrasion mills, and Alex Simms and Laura Reynolds for assistance with mud particle size analysis. We thank Charlie Kerans and an anonymous reviewer for their constructive comments. This project was supported by an American Chemical Society Petroleum Research Fund Grant 56757-ND8 (to W. W. F.). E. J. T. was supported by an Agouron Geobiology Postdoctoral Fellowship. Experiment parameters and results are provided in the supporting information. Matlab code for the abrasion mud production model (including code to generate Figures 1 and 3) and advection length scale calculations (v.1.0.0) is archived (https://doi.org/10.5281/zenodo.2177107).

References

Atkinson, M. J., & Bingman, C. (1997). Elemental composition of commercial seasalts. *Journal of Aquariculture and Aquatic Sciences*, *8*(2), 39–43.

Bathurst, R. G. C. (1975). Carbonate sediments and their diagenesis. In *Developments in Sedimentology* (Vol. 12). Amsterdam: Elsevier Publishing Co.

Beaupré, S. R., Roberts, M. L., Burton, J. R., & Summons, R. E. (2015). Rapid, high-resolution ^{14}C chronology of ooids. *Geochimica et Cosmochimica Acta*, *159*, 126–138.

Broecker, W. S., Sanyal, A., & Takahashi, T. (2000). The origin of Bahamian whitings revisited. *Geophysical Research Letters*, *27*(22), 3759–3760.

Broecker, W. S., & Takahashi, T. (1966). Calcium carbonate precipitation on the Bahama Banks. *Journal of Geophysical Research*, *71*(6), 1575–1602.

Cloud, P. E., Blackmon, P. D., Sisler, F. D., Kramer, H., Carpenter, J. H., Robertson, E. C., et al. (1962). *Environment of Calcium Carbonate Deposition West of Andros Island, Bahamas, With Sections on Mechanical Characteristics of the Sediments; Microbiology and Biochemistry of Sediments and Overlying Water; Chemical Analyses of the Water: The Problem of Calcium Determination in sea Water and Experimental Consolidation of Calcium Carbonate Sediment; Environment of Calcium Carbonate Deposition West of Andros Island*. Washington : U.S: US Govt. Print. Off.

Davies, P. J., Bubela, B., & Ferguson, J. (1978). Formation of ooids. *Sedimentology*, *25*(5), 703–730.

Debenay, J.-P., André, J.-P., & Lesourd, M. (1999). Production of lime mud by breakdown of foraminiferal tests. *Marine Geology*, *157*(3), 159–170.

Dierrsen, H. M., Zimmerman, R. C., & Burdige, D. J. (2009). Optics and remote sensing of Bahamian carbonate sediment whitings and potential relationship to wind-driven Langmuir circulation. *Biogeosciences*, *6*(3).

Dietrich, W. E. (1982). Settling velocity of natural particles. *Water Resources Research*, *18*(6), 1615–1626.

Dravis, J. J., & Wanless, H. R. (2017). Impact of strong easterly trade winds on carbonate petroleum exploration-Relationships developed from Caicos Platform, southeastern Bahamas. *Marine and Petroleum Geology*, *85*, 272–300.

Duguid, S. M. A., Kyser, T. K., James, N. P., & Rankey, E. C. (2010). Microbes and ooids. *Journal of Sedimentary Research*, *80*(3), 236–251. https://doi.org/10.2110/jsr.2010.027

Farrow, G. E., & Fyfe, J. A. (1988). Bioerosion and carbonate mud production on high-latitude shelves. *Sedimentary Geology*, *60*(1–4), 281–297.

Ford, M. R., & Kench, P. S. (2012). The durability of bioclastic sediments and implications for coral reef deposit formation. *Sedimentology*, *59*(3), 830–842. https://doi.org/10.1111/j.1365-3091.2011.01281.x

Ganti, V., Lamb, M. P., & McElroy, B. (2014). Quantitative bounds on morphodynamics and implications for reading the sedimentary record. *Nature Communications*, *5*, 1–7.

Garcia, M., & Parker, G. (1991). Entrainment of bed sediment into suspension. *Journal of Hydraulic Engineering*, *117*(4), 414–435.

Gischler, E., Dietrich, S., Harris, D., Webster, J. M., & Ginsburg, R. N. (2013). A comparative study of modern carbonate mud in reefs and carbonate platforms: Mostly biogenic, some precipitated. *Sedimentary Geology*, *292*, 36–55. https://doi.org/10.1016/J.SEDGEO.2013.04.003

Gischler, E., & Zingeler, D. (2002). The origin of carbonate mud in isolated carbonate platforms of Belize, Central America. *International Journal of Earth Sciences*, *91*(6), 1054–1070. https://doi.org/10.1007/s00531-002-0288-5

Gonzalez, R., & Eberli, G. P. (1997). Sediment transport and bedforms in a carbonate tidal inlet; Lee Stocking Island, Exumas, Bahamas. *Sedimentology*, *44*(6), 1015–1030.

Grant, W. D., & Madsen, O. S. (1982). Movable bed roughness in unsteady oscillatory flow. *Journal of Geophysical Research*, *87*(C1), 469–481.

Grotzinger, J. P., & James, N. P. (2000). Precambrian carbonates: Evolution of understanding. In J. P. Grotzinger & N. P. James (Eds.), *Carbonate Sedimentation and Diagenesis in the Evolving Precambrian WorldSociety of Economic Paleontologists and Mineralogists, Special Publication* (Vol. 65, pp. 179–205).

Hallock, P. (1988). The role of nutrient availability in bioerosion: Consequences to carbonate buildups. *Palaeogeography, Palaeoclimatology, Palaeoecology*, *63*(1–3), 275–291.

Harris, P. M. M., Purkis, S. J., Ellis, J., Swart, P. K., & Reijmer, J. J. G. (2015). Mapping bathymetry and depositional facies on Great Bahama Bank. *Sedimentology*, *62*(2), 566–589.

Kench, P. S. (1998). A currents of removal approach for interpreting carbonate sedimentary processes. *Marine Geology*, *145*(3–4), 197–223.

Lamb, M. P., Dietrich, W. E., & Sklar, L. S. (2008). A model for fluvial bedrock incision by impacting suspended and bed load sediment. *Journal of Geophysical Research*, *113*, F03025. https://doi.org/10.1029/2007JF000915

Le Bouteiller, C., Naaim-Bouvet, F., Mathys, N., & Lavé, J. (2011). A new framework for modeling sediment fining during transport with fragmentation and abrasion. *Journal of Geophysical Research*, *116*, F03002. https://doi.org/10.1029/2010JF001926

Leeder, M. R. (1979). "Bedload"dynamics: Grain-grain interactions in water flows. *Earth Surface Processes*, *4*(3), 229–240.

Lowenstam, H. A. (1955). Aragonite needles secreted by algae and some sedimentary implications. *Journal of Sedimentary Research*, *25*(4).

Macintyre, I. G., & Reid, R. P. (1992). Comment on the origin of aragonite needle mud: A picture is worth a thousand words. *Journal of Sedimentary Research*, *62*(6).

Milliman, J. D., Freile, D., Steinen, R. P., & Wilber, R. J. (1993). Great Bahama Bank aragonitic muds: Mostly inorganically precipitated, mostly exported. *Journal of Sedimentary Research*, *63*(4).

Morse, J. W., Gledhill, D. K., & Millero, F. J. (2003). $CaCO_3$ precipitation kinetics in waters from the great Bahama bank: Implications for the relationship between bank hydrochemistry and whitings. *Geochimica et Cosmochimica Acta*, *67*(15), 2819–2826.

Nelsen, J. E., & Ginsburg, R. N. (1986). Calcium carbonate production by epibionts on Thalassia in Florida Bay. *Journal of Sedimentary Research*, *56*(5).

Neumann, A. C., & Land, L. S. (1975). Lime mud deposition and calcareous algae in the Bight of Abaco, Bahamas: A budget. *Journal of Sedimentary Research*, *45*(4).

Palacas, J. G., Anders, D. E., & King, J. D. (1984). South Florida Basin—A prime example of carbonate source rocks of petroleum. In *Petroleum Geochemistry and Source Rock Potential of Carbonate Rocks* (pp. 71–96). Tulsa, OK: AAPG (American Association of Petroleum Geologists).

Pomar, L., & Hallock, P. (2008). Carbonate factories: A conundrum in sedimentary geology. *Earth-Science Reviews*, *87*(3–4), 134–169.

Purkis, S., Cavalcante, G., Rohtla, L., Oehlert, A. M., Harris, P. M., & Swart, P. K. (2017). Hydrodynamic control of whitings on Great Bahama Bank. *Geology*, *45*(10), 939–942. https://doi.org/10.1130/G39369.1

Rankey, E. C., & Reeder, S. L. (2010). Controls on platform-scale patterns of surface sediments, shallow Holocene platforms, Bahamas. *Sedimentology*, *57*(6), 1545–1565.

Rankey, E. C., Riegl, B., & Steffen, K. (2006). Form, function and feedbacks in a tidally dominated ooid shoal, Bahamas. *Sedimentology*, *53*(6), 1191–1210.

Robbins, L. L., & Blackwelder, P. L. (1992). Biochemical and ultrastructural evidence for the origin of whitings: A biologically induced calcium carboante precipitation mechanism. *Geology*, *20*(5), 464–468.

Robbins, L. L., Tao, Y., & Evans, C. A. (1997). Temporal and spatial distribution of whitings on Great Bahama Bank and a new lime mud budget. *Geology*, *25*(10), 947–950.

Scheingross, J. S., Brun, F., Lo, D. Y., Omerdin, K., & Lamb, M. P. (2014). Experimental evidence for fluvial bedrock incision by suspended and bedload sediment. *Geology*, *42*(6), 523–526.

Schieber, J., Southard, J. B., Kissling, P., Rossman, B., & Ginsburg, R. (2013). Experimental deposition of carbonate mud from moving suspensions: Importance of flocculation and implications for modern and ancient carbonate mud deposition. *Journal of Sedimentary Research*, *83*(11), 1025–1031.

Shinn, E. A., Steinen, R. P., Lidz, B. H., & Swart, P. K. (1989). Whitings: A sedimentologic dilemma. *Journal of Sedimentary Petrology*, *59*(1), 147–161. https://doi.org/10.1306/212F8F3A-2B24-11D7-8648000102C1865D

Sklar, L. S., & Dietrich, W. E. (2001). Sediment and rock strength controls on river incision into bedrock. *Geology*, *29*(12), 1087–1090.

Sklar, L. S., & Dietrich, W. E. (2004). A mechanistic model for river incision into bedrock by saltating bed load. *Water Resources Research*, *40*, W06902. https://doi.org/10.1029/2012WR012267

Sorby, H. C. (1879). The structure and origin of limestones. *Proceedings of Geological Society of London*, *35*, 56–95.

Stockman, K. W., Ginsburg, R. N., & Shinn, E. A. (1967). The production of lime mud by algae in south Florida. *Journal of Sedimentary Research*, *37*(2).

Trower, E. J., Cantine, M. D., Gomes, M. L., Grotzinger, J. P., Knoll, A. H., Lamb, M. P., et al. (2018). Active ooid growth driven by sediment transport in a high-energy shoal, Little Ambergris Cay, Turks and Caicos Islands. *Journal of Sedimentary Research*, *88*, 1132–1151.

Trower, E. J., Lamb, M. P., & Fischer, W. W. (2017). Experimental evidence that ooid size reflects a dynamic equilibrium between rapid precipitation and abrasion rates. *Earth and Planetary Science Letters*, *468*, 112–118. https://doi.org/10.1016/j.epsl.2017.04.004

Yates, K. K., & Robbins, L. L. (1998). Production of carbonate sediments by a unicellular green alga. *American Mineralogist*, *83*(11), 1503–1509.